Chapter 2 Theory

2.1 Huygens' integral and ABCD law

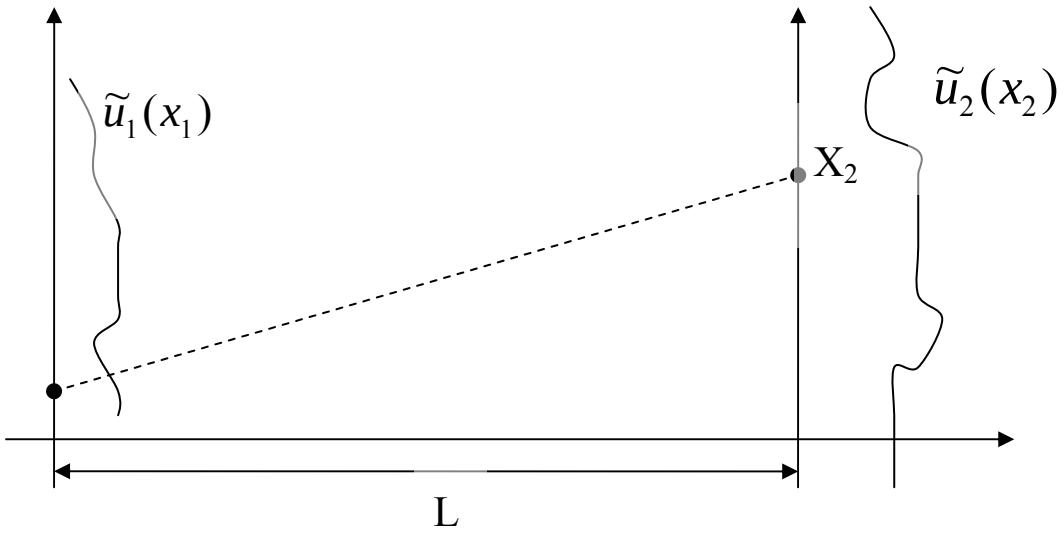

Fig. 2.1 Huygens' integral in free space

In this section, we introduce the Huygens' integral and the ABCD law which we will use in our simulation model. For simplicity we will discuss it in one-dimension and then extend to deal with the laser system with cylindrical symmetry. Huygens' integral in one transverse dimension for propagation through a distance L in free space can be written in the form

$$\tilde{u}_2(x_2) = e^{-jkL}\int_{-\infty}^{\infty}\tilde{K}(x_2,x_1)\tilde{u}(x_1)dx_1$$

$$= \sqrt{\frac{j}{L\lambda}}\int_{-\infty}^{\infty}\tilde{u}_1(x_1)\exp[-jk\rho(x_1,x_2)]dx_1$$

where the path length $\rho(x_1,x_2)$ for an optical ray in free space traveling from position x_1 at plane z_1 to position x_2 at plane $z_2 = z_1+L$ is given by the paraxial approximation

$$\rho(x_1,x_2) = \sqrt{L^2+(x_2-x_1)^2} \approx L + \frac{(x_2-x_1)^2}{2L}.$$

So, the Huygens-Fresnel kernel for wave propagation in free space thus takes on the

form

$$\widetilde{K}(x_2, x_1) = \sqrt{\frac{j}{L\lambda}} \exp[-j\frac{\pi(x_2 - x_1)^2}{L\lambda}]$$

in one transverse dimension, or a product of two such kernel in two transverse dimensions.

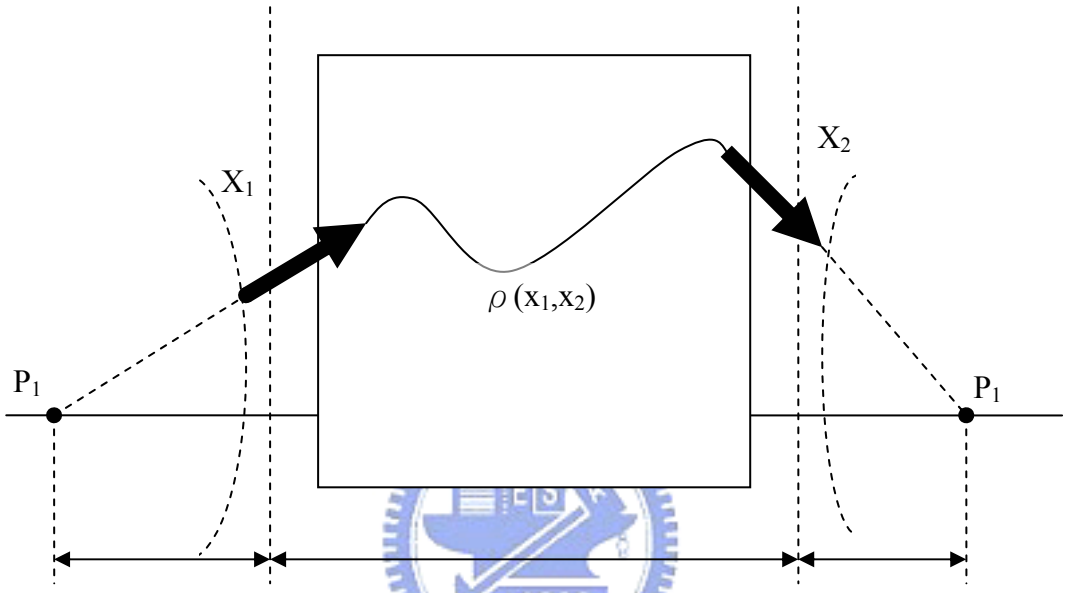

Fig. 2.2 Fermat's principle says the total path length from P_1 to P_2 must be the same along the axis or along the ray path indicated by the dashed lines

Consider instead an input wavefunction $\widetilde{u}_1(x)$ travels not through free space, but through a cascade optical system containing an arbitrary collection of real paraxial optical elements between the two planes $z_1$and z_2, as illustrate in Fig. 2.2. If a ray enters at a specified point x_1 and exits at another point x_2, then from the ray relationship $x_2 = Ax_1+Bx_1'$. And the input slope of this particular ray must be given by $x_1' = \frac{x_2 - Ax_1}{B}$ and the exit slope must be $x_2' = \frac{Dx_2 - x_1}{B}$. The input ray may then be viewed as coming from an on-axis source point P_1 located a distance R_1 behind the input plane. Hence $R_1$is given by

$$\frac{R_1}{n_1} \equiv \frac{x_1}{x_1'} = \frac{Bx_1}{x_2 - Ax_1}.$$

Similarly,

$$\frac{R_2}{n_2} \equiv \frac{x_2}{x_2'} = \frac{Bx_1}{Dx_2 - x_1}.$$

This output ray thus intersects the axis at point P_2 located a distance R_2 behind the plane z_2. We now have both R_1 and R_2 given in terms of x_1, x_2,and the ABCD matrix elements.

But Fermat's principle says that "all rays connecting two conjugate points must have the same optical path length between these two points," It means that the ray path from P_1 to P_2 through x_1 and $x_2$is equal to the ray path from P_1 to P_2 along the optical axis. The total optical path length along the optical axis from point P_1 to P_2 is given by

$$P_1P_2 \equiv n_1R_1 + L_0 - n_2R_2,$$

where the minus sign is associated with the sign convention for R_2. The total distance going along the off-axis ray through points X_1 and X_2 is given, in the paraxial approximation, by

$$\begin{aligned} P_1X_1X_2P_2 &= P_1X_1 + X_1X_2 + X_2P_2 \\ &= n_1\sqrt{R_1^{\,2} + x_1^{\,2}} + \rho(x_1, x_2) - n_2\sqrt{R_2^{\,2} + x_2^{\,2}} \\ &\approx n_1\left(R_1 + \frac{x_1^{\,2}}{2R_1}\right) + \rho(x_1, x_2) - n_2\left(R_2 + \frac{x_2^{\,2}}{2R_2}\right) \end{aligned}$$

The Fermat's principle requires that the total path length from point P_1 to the conjugate point P_2 going along either path be the same, i.e., $P_1P_2 = P_1X_1X_2P_2$, it gives the desired eikonal function

$$\rho(x_1, x_2) = L_0 - \frac{n_1 x_1^{\,2}}{2R_1} + \frac{n_2 x_2^{\,2}}{2R_2} = L_0 + \frac{1}{2B}(Ax_1^{\,2} - 2x_1 x_2 + Dx_2^{\,2}) .$$

Thus, the Huygens' integral for wave propagation all the way through the entire paraxial system can be written as,

$$\tilde{u}_2(x_2) = e^{-jkL_0} \int_{-\infty}^{\infty} \tilde{K}(x_2, x_1)\tilde{u}(x_1)dx_1 ,$$

with the Huygens kernel in one transverse dimension being given by

$$\tilde{K}(x_2, x_1) = \sqrt{\frac{j}{B\lambda_0}} \exp[-j\frac{\pi}{B\lambda_0}(Ax_1^{\,2} - 2x_1 x_2 + Dx_2^{\,2})] .$$

We knew the relation between the Huygens' integral and ABCD law in one-dimension. But the real system is two-dimension with cylindrical symmetry, it can be simplified to an one-dimension case and the Huygens' integral becomes

$$E_{m+1}^{-}(r) = -\frac{2\pi j}{B\lambda}\int_0^{\infty} \exp(j\frac{2\pi 2L}{\lambda m} + j\Delta\phi(r'))E_m^{+}(r')\exp\{(\frac{j\pi}{B\lambda})(Ar'^2 + Dr^2)\}J_0(\frac{2\pi rr'}{B\lambda})r'dr' .$$

2.2 Thermal effect

The other important effect in solid state laser is the thermal optic effect. This effect results from temperature induced change of in the refractive index of the gain medium. In order to model the thermally induced index changes, the heat transfer equation must be solved for the laser medium to obtain an appropriate temperature distribution. In this work, an approximate analytic solution to the heat transfer equation are developed for cw, axially symmetric, longitudinal pumping of a cylindrically symmetric solid state laser rod with conductive boundary condition.

Consider a model consists of a solid state laser rod longitudinally pumped by a second cw laser, as shown in Fig. 2.3, that shows side view and end view of a laser rod and heat sink. The periphery of the laser crystal is held at constant temperature

by an actively cooled heat sink. In the steady state

$$\nabla \bullet \vec{h}(r,z) = Q(r,z), \tag{1}$$

where $\vec{h}(r,z)$ is the heat sink, and $Q(r,z) = dP(r,z)/dV$ is the power per unit volume deposited as in the laser crystal. The heat flux is related to the corresponding temperature distribution within the crystal by

$$h(r,z) = -K_c \nabla T(r,z), \tag{2}$$

where K_c is the thermal conductivity of the laser material.

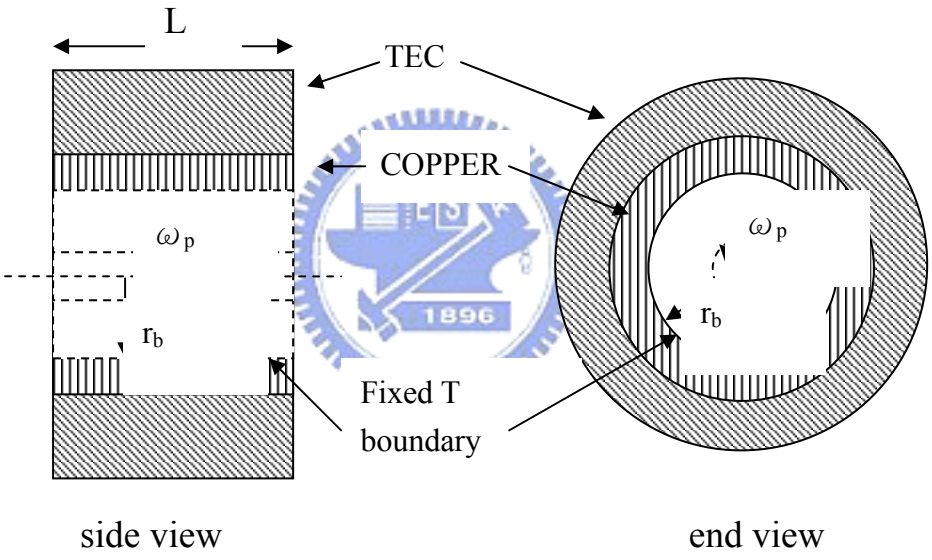

Fig. 2.3 Side view and end view of an applicable laser rod and thermoelectrically cooled (TEC) heat sink. The length of the rod is L, the rod radius is r_b, and the $1/e^2$ radius of the Gaussian pump beam is ω_p.

Consider the case where the thermal conductivity of the heat sink is much greater than the thermal conductivity of the laser crystal. For example, the thermal conductivity of Cu, a common heat sink material, is a factor of 30 larger than that of yttrium aluminum garnet (YAG), a common solid state laser material. If it is

assumed that the heat flow is essentially radial, Eq. (1) can be integrated over a crystal volume bounded by a Gaussian surface of radius r and infinitesimal thickness Δz. This yields

$$2\pi r\Delta z h = \int_z^{z+\Delta z} \int_0^r \frac{dP(r',z')}{dV} 2\pi r' dr' dz' \,. \tag{3}$$

Now

$$\frac{dP(r,z)}{dV} = \alpha I_h(r,z) \,, \tag{4}$$

where α is the absorption coefficient of the material and $I_h(r,z)$ is the intensity of the incident pump light that results in heating of the crystal. Here, it is assumed that

$$I_h(r,z) = I_{0h} \exp(-\frac{2r^2}{\omega_p{}^2}) \exp(-\alpha z) \,. \tag{5}$$

In Eq. (5), I_{0h} is the incident heat irradiance on axis and ω_p is the $1/e^2$ Gaussian radius of the pump beam. Substituting Eqs. (4) and (5) into Eq. (3) and performing the integration yields

$$h(r,z) = (\frac{\alpha P_{ph}}{2\pi}) \exp(-\alpha z)(\frac{1-\exp(-2r^2/\omega_p{}^2)}{r}) \,, \tag{6}$$

where $P_{ph} = \pi\omega_p I_{0h}/2$ is the fraction of pump power that results in heating. Substituting Eq. (6) into Eq. (2), we can obtain

$$\Delta T(r',z) = -\frac{1}{K_c} \int_r^{r_b} \frac{\alpha\xi P_{abs}}{2\pi} \exp(-\alpha z) \frac{1-\exp(-2r^2/\omega_p{}^2)}{r} dr \,, \tag{7}$$

where the additional coefficient ξ is the fractional thermal loading and P_{abs} is the absorbed pump power.

The total phase change ΔΦ that is accumulated by the laser light for a single pass through the laser rod is given by

$$\Delta\phi(r) = \int_0^l k\Delta n(r,z)dz \,, \tag{8}$$

where Δn(r,z) is the change in refractive index of the laser medium resulting from temperature effects, and l is the length of the laser rod. Changes in the index of refraction (n) accrue from three temperature-dependent effects: thermal variations of the index due to dn/dT

$$\Delta n(r,z)_T = \Delta T(r,z)(\frac{dn}{dT}) \,, \tag{9}$$

thermal induced stress and thermal deformation of the rod. In flashlamp pumped YAG, the variation of n due to dn/dT accounts for 74% of the thermally induced focusing. Substituting Eq. (9) to Eq. (8), we can obtain the relation between the temperature and the changes of the phase

$$\Delta\phi(r') = \int_0^l k\Delta T(r',z)\frac{dn}{dT}dz \,. \tag{10}$$

2.3 Simulation model

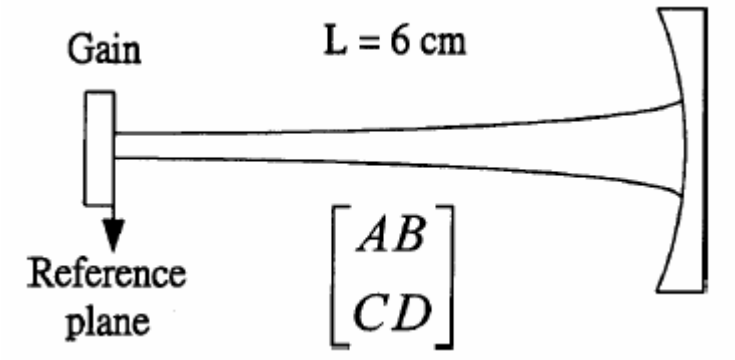

Fig. 2.4 Configuration of the laser system.

Consider the laser system shown in Fig. 2.4. Let the reference plane be where the light beam just leaves the laser crystal toward the curved mirror. In cylindrical symmetry, propagation of the light field toward the curved mirror and back to the flat mirror according to the generalized Huygens diffraction integral is

$$E_{m+1}^{-}(r) = -\frac{2\pi j}{B\lambda}\int_0^{\infty} \exp(j\frac{2\pi 2L}{\lambda m} + j\Delta\phi(r'))E_m^{+}(r')\exp\{(\frac{j\pi}{B\lambda})(Ar'^2 + Dr^2)\}J_0(\frac{2\pi rr'}{B\lambda})r'dr', \quad (1)$$

with round trip transmission matrix M = $\begin{bmatrix} A & B \\ C & D \end{bmatrix}$, which has discussed in the section 2.1. Here $E_m^{+}(r')$ and $E_{m+1}^{-}(r')$ are the electric fields of the mth and (m+1)st round trips at the planes immediately after and before the gain medium (denoted by the superscripts + and -); r' and r are the corresponding radial coordinates, λ is the wavelength of the laser, and J_0 is a Bessel function of zero-order. We have imposed the phase shift ΔΦ induced by thermal lens effect in the diffraction integral. The phase shift is given (ref. [8]) by

$$\Delta\phi(r') = \int_0^l k\Delta T(r', z)\frac{dn}{dT}dz,$$

where $\Delta T(r', z) = -\frac{1}{K_c}\int_r^{r_b} \frac{\alpha\xi P_{abs}}{2\pi}\exp(-\alpha z)\frac{1-\exp(-2r^2/\omega_p{}^2)}{r}dr$ is the temperature difference between the calculated point (r', z) and the boundary point (rb, z), ξ is the fractional thermal loading, P_{abs} is the absorbed pump power, z is the axial coordinate, and rb, d, α, K_c, and dn/dT are the radius, thickness, absorption coefficient, thermal conductivity, and the thermal-optic coefficient of the laser crystal, respectively. Note that the distribution of the thermal induced stress and the thermal deformation of the crystal were neglected and the conventional edge cooling was assumed. In a thin-slab approximation, we can relate the electric fields E_{m+1}^{+} to E_{m+1}^{-} (after and before the gain medium) in the same round trip as

$$E_{m+1}^{+}(r) = \rho E_{m+1}^{-}(r)\exp(\sigma\Delta N d)\prod(r/a) \quad (3)$$

where $1-\rho^2$ is the round-trip energy loss, σ is the stimulated-emission cross section, ΔN is the population inversion per unit volume, d is the length of the active medium, and ∏(r/a) is an aperture function that equals 1 for r less than aperture radius a and equals 0 otherwise. Furthermore, assuming that the evolution of the population

inversion follows the rate equation of a four-level system, we can write the rate equation as

$$\Delta N_{m+1} = \Delta N_m + R_{pm}\Delta t - \gamma \Delta N_m \Delta t - \frac{|E_m|^2}{E_s{}^2}\Delta N_m \Delta t \,, \qquad (4)$$

where R_{pm} is the pumping rate (per unit time per unit volume), t is the round trip time, E_s is the saturation parameter of the active medium, and γ the spontaneous decay rate, and N_0 is the total density of the active medium. This method was used to model a single-longitudinal multitransversal high-power solid-state ring laser (ref. [5-7]) and to analyze the decay rate of standing-wave laser cavities in the linear regime (ref. [9]). It was found that a standing-wave resonator can be approximated by a ring resonator if a thin gain medium is placed close to one of the end mirrors (ref. [10]). For a continuous

Gaussian pump profile $R_{pm} = R_{p0}\exp(-2r^2/2\omega_p{}^2)$ with constant pumping beam radius ω_p throughout the active medium (thin slab), the total pumping rate over the entire active medium is

$$\int R_{pm} dV = P_p / h\upsilon_p \,, \qquad (4)$$

where P_p is the effective pumping power and $h\nu_p$ is the photon energy of the pumping laser. Because we considered only single-longitudinal-mode dynamics, we have omitted the dispersion of the active medium, so the gain is assumed to be real. Therefore we have four control parameters: ρ, R, wp, and Pp, which play important roles in the laser system and are investigated in detail as follows.

In an ordinary axially pumped solid-state laser, the round-trip propagation time is many orders of magnitude shorter than the spontaneous decay time, especially in a short cavity. As a result, it would take a large number of iterations to arrive at the final state (which may be stable or unstable). To reduce computation time and

because the quasi-periodic bifurcation point is just above the stable continuous-wave solution, we used the scaling method (ref. [9]) to magnify g by 10^4 times to determine the bifurcation points. We also checked some important points without scaling that showed no promising change in the quasi-periodic threshold. To reduce the influence of the diffraction loss, we slightly varied R of the curved mirror rather than changing cavity length L to simulate tuning the laser cavity across the point of degeneration.